ORIGINAL ARTICLE

GPS snow sensing: results from the EarthScope Plate Boundary Observatory

Kristine M. Larson · Felipe G. Nievinski

Abstract Accurate measurements of snowpack are needed both by scientists to model climate and by water supply managers to predict/mitigate drought and flood conditions. Existing in situ snow sensors/networks lack the necessary spatial and temporal sensitivity. Satellite measurements currently assess snow cover rather than snow depth. Existing GPS networks are a potential source of new snow data for climate scientists and water managers which complements existing snow sensors. Geodetic-quality GPS networks often provide signal-to-noise ratio data that are sensitive to snow depth at scales of $\sim 1,000$ m^2, a much larger area than for other in situ sensors. However, snow depth can only be estimated at GPS sites when the modulation frequency of multipath signals can be resolved. We use data from the EarthScope Plate Boundary Observatory to examine the potential for snow sensing in GPS networks. Examples are shown for successful and unsuccessful snow retrieval sites. In particular, GPS sites in forested regions typically cannot be used for snow sensing. Multiple-year time series of snow depth are estimated from GPS sites in the Rocky Mountains. Peak snow depths ranged from 0.4 to 1.2 m. Comparisons with independent sensors show strong correlations between the GPS snow depth estimates and the timing of snowstorms in the region.

Keywords GPS · Reflections · Multipath · Snow

K. M. Larson (✉) · F. G. Nievinski
Department of Aerospace Engineering Sciences, University of Colorado, Boulder, Boulder, CO 80309-0429, USA
e-mail: Kristinem.larson@gmail.com

Introduction

In the past 20 years, scientists and surveyors have installed thousands of GPS receivers around the world. The density and location of these GPS sites depend very much on the purpose of the network. The common features of these GPS networks include continuous operation, free daily data access to the community via the Internet, geodetic-quality receiver and antennas, some form of engineering support to maintain the networks, and telemetry/archiving systems. Although atmospheric research is an important scientific partner in GPS, the majority of these networks were installed for positioning applications. As telecommunications costs have been lowered, some of these networks have begun operating at higher sampling rates and in real time.

Although geodetic-quality GPS sites have much in common, they intrinsically differ in terms of their local multipath environment. For example, many EUREF sites (Europe, http://epncb.oma.be/) are located in urban areas. Multipath effects in GPS data from this kind of network are often dominated by reflections from buildings, streets, and other man-made surfaces. Many of the SCIGN GPS sites (Southern California, http://www.scign.org/) were similarly situated in high-density population centers. In contrast, the majority of EarthScope Plate Boundary Observatory (http://pbo.unavco.org) GPS sites are located in rural areas (Fig. 1; Table 1). Multipath errors from PBO sites are dominated by nearby soil surfaces, vegetation, and seasonal snow pack. Changes in multipath characteristics at these sites, both on seasonal and weekly time scales, provide an opportunity to assess water transport at hundreds of existing sites. They could also be used to validate current and future space-borne sensors. Of the water cycle effects evident in GPS multipath data, snow depth is both the
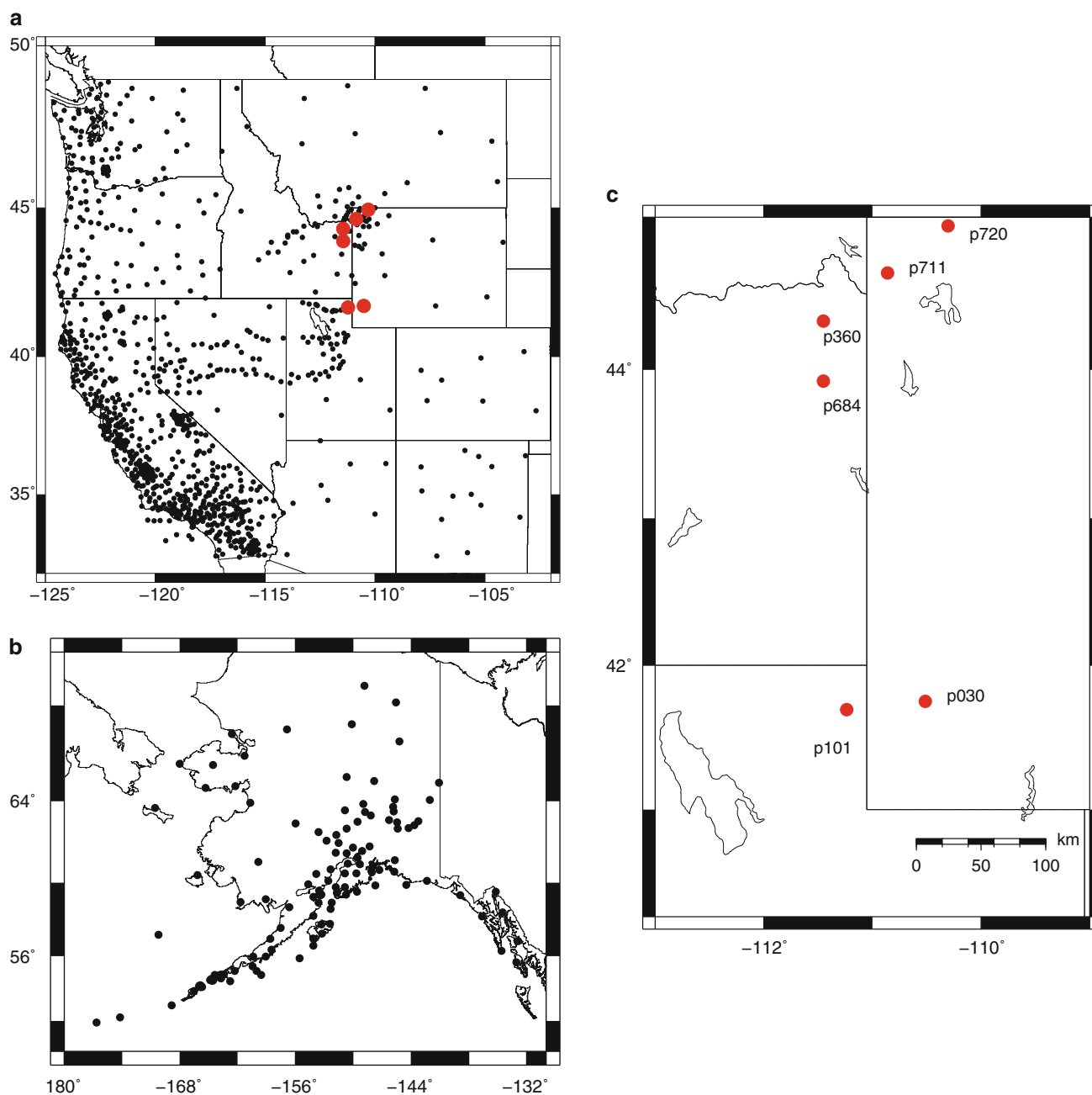
Fig. 1 a, **b** PBO network sites in the western United States and Alaska; **c** location of PBO stations described in this paper. Site coordinates are given in Table 1

Table 1 PBO station locations

Station	Latitude degrees	Longitude degrees	Elevation meters	State
p030	41.749815	−110.512810	2,149.8	Wyoming
p101	41.692274	−111.236016	2,016.1	Utah
p360	44.317852	−111.450677	1,857.9	Idaho
p684	43.919149	−111.450486	1,693.9	Idaho
p711	44.635565	−110.861066	2,118.7	Wyoming
p720	44.943101	−110.306257	1,924.0	Wyoming

largest and the most straightforward to model. Our focus is to demonstrate how to extract snow depth estimates from geodetic GPS networks, using the PBO data as a test case. Previous studies of geodetic GPS snow sensing were limited to several days or a single site. In particular, Larson et al. (2009) used a single site that had almost no terrain relief and few "real-world" obstructions. Ozeki and Heki (2012) examined a longer time period, but also only at a single site. More recent work addressed a GPS site that was installed specifically for the purpose of snow sensing (Gutmann et al. 2011). PBO data will be used to demonstrate the path forward for leveraging existing GPS positioning networks into networks that also provide snow measurements. In addition to reviewing the principles associated with GPS snow sensing, implementation of the method will be emphasized, along with examples of when the method works and when it fails.

Snow measurements in the United States

Snow generally has a negative connotation in the geodetic community, mostly stemming from the experience that buildup of snow and ice-rime on antennas biases position estimates (Jaldehag et al. 1996). At the same time that the geodetic community has been seeking "solutions" to the snow problem, for example, via heating of the antenna, the cryospheric community has actively been seeking new sensors to measure snow depth and snow water equivalent, SWE (the amount of water stored in snowpack). These measurements of snow are needed to model both regional and global climate systems. These data are also needed for forecasting the rate of snowmelt, so that flood hazards and water supply can be managed. In the United States, snow is monitoring in a variety of ways. The Snowpack Telemetry (SNOTEL) network (Serreze et al. 1999) measures SWE using fluid-filled steel pillows and, more recently, snow depth using sonic sensors. It has excellent temporal resolution (hourly), but is limited spatially to ~ 10 m^2 for SWE, and even smaller areas for snow depth. Since SNOTEL sensors provide only a few and sparse point-like measurements, they cannot represent the variation of snow in, for example, a basin (Molotch and Bales 2006).

Limitations in the footprint of existing sensors are compounded by the spatial variability exhibited by snow. Its deposition is heterogeneous, with generally greater amounts of snow falling at higher elevations (Seyfried and Wilcox 1995). Once on the ground, the snow is also impacted (and redistributed) by wind (Kind 1981) or avalanching and sloughing (Elder et al. 1991; Bloschl et al. 1991). Furthermore, snowpack ablation is also nonuniform because it is controlled by spatially and temporally varying parameters such as temperature, wind, and radiation

(Erickson et al. 2005). This translates into snow changing by several tens of centimeters in depth over a few meter horizontal distances.

In addition to continuously operating point sensors like SNOTEL, more than 2,000 snow courses in the western United States are measured each year. Snow courses sample a ~ 100-m transect at each site. Unfortunately, data are only collected once a month. This limits the value of these networks for useful information about the dynamics of snow accumulation and melt. Ideally snow pack would be monitored from space. However, no operational satellite provides either snow depth or SWE at the necessary temporal and spatial scales—with experimental systems being tested (Armstrong and Brodzik 2002) and new ones being proposed (ESA 2008)—nor are airborne remote-sensing platforms routinely used in the United States.

In summary, there is no one snow-sensing system that provides the spatial and temporal sampling desired by climate modelers and water managers. There is need for additional snow sensors that measure snow properties over larger areas and at more numerous locations than the SNOTEL network. Geodetic-quality GPS systems were certainly not designed to be snow sensors, and thus, they have limitations in how they can contribute to monitoring of snowpack. From a positive perspective, they have sensing zones that are typically two orders of magnitude larger than SNOTEL and are already deployed in large quantities; furthermore, the geodetic community has demonstrated that general GPS technology operates well under harsh winter conditions. By extracting snow depth information from existing and freely available GPS data, a new source of inexpensive snow information becomes available to a broader scientific community; conversely, snow sensing adds value to existing GPS networks.

GPS data issues

Snow sensing utilizes signal-to-noise ratio (SNR) observations. GPS data from geodetic networks are generally made available to the public in an ASCII format called RINEX (Receiver Independent Exchange format). Although the L1 and L2 carrier phases (and pseudorange) are the primary observables used by geodesists and surveyors, many network operators also archive the so-called S1 and S2 observables, referred to as signal strength in the RINEX specifications. Standardized RINEX S1/S2 would correspond to the quantity called carrier-to-noise-density ratio (C/N$_0$), the ratio of signal power to the noise power spectral density. SNR is related to C/N$_0$ through the noise bandwidth (B) as in SNR $=$ (C/N$_0$)/B (Joseph 2010), thus having units of decibels (in logarithmic scale) or watts per watt (in linear scale—sometimes in volts per volt when

taking the square root). For simplicity, S1/S2 observations will be reported as SNR, assuming a 1-Hz bandwidth, and volts when converted to a linear scale.

Figure 2a shows the general features of SNR data from a code-correlating receiver. In the absence of multipath, SNR values smoothly rise from ~ 35 dB to a peak of ~ 52 dB. This trend is a consequence primarily of the direct or line-of-sight power (P_d) and secondarily the reflected power (P_r):

$$SNR \propto P_d + P_r + \sqrt{P_d P_r} \cos \phi. \tag{1}$$

It is determined by the satellite transmitted power and by the antenna gain pattern, and whether the receiver is using code-enabled tracking methods. Superimposed on this trend, modulations are seen at the rising end of the arc; these peaks and troughs are constructive and destructive interference caused by coherent multipath, dictated by the reflection phase (ϕ).

The frequency, phase, and amplitude of the multipath modulations are caused by a variety of factors, including the composition, geometry, and roughness of the reflecting surface. Since the trend is not of interest, a low-order polynomial is typically fit to the data to remove it. More complicated detrending schemes have also been suggested
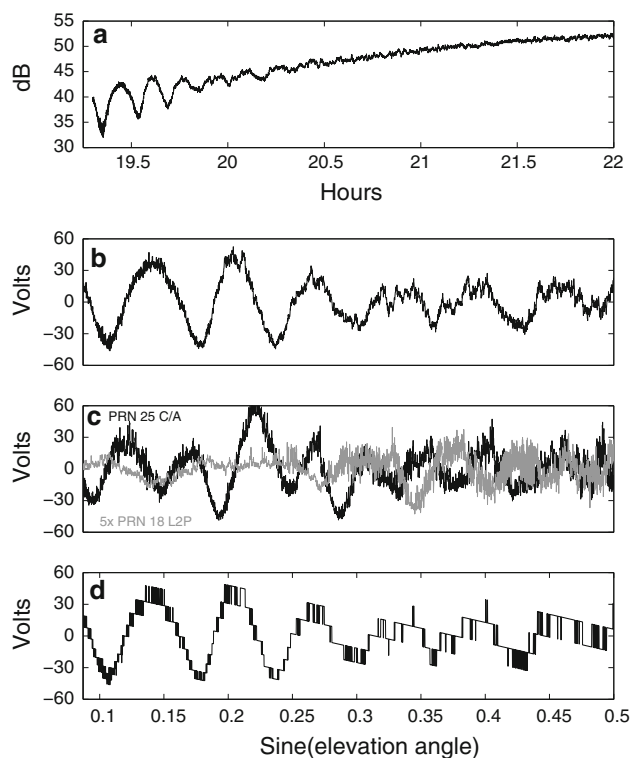
(Bilich and Larson 2007), but these have not been shown to improve the retrieval of multipath modulation frequencies. The modulations seen in Fig. 2b are typical for a "strong" ground reflector for an antenna ~ 2 m above the ground. The amplitude of the modulation decreases as the satellite rises and its elevation angle increases; although somewhat exacerbated by the logarithmic scale, this is primarily due to the antenna gain pattern, which does a better job of suppressing multipath at higher elevation angles. At lower elevation angles, reflections off dielectric surfaces do not suffer as much polarization reversal, therefore even geodetic-quality antennas subject near-grazing snow reflections to as much gain as the direct signal.

The data shown in Fig. 2a and b are from the new L2C signal, and thus, the SNR is higher than it would be for a signal that used less optimal correlation techniques. For comparison, data are also shown from the C/A and L2-P(Y) channels (Fig. 2c). It is clear that both are significantly noisier than the L2C SNR data. Although a periodic signal is visible in the L2-P(Y) SNR data, the amplitude is much smaller than in C/A or L2C (Ozeki and Heki 2012). This will always be the case for a receiver that is not using the known PRN code in its tracking loop (Woo 1999), that is, for as long as anti-spoofing is enabled. As for using C/A SNR data for snow sensing, being a much shorter code than both L2C and P(Y), it is prone to cross-channel self-interference, especially from stronger, higher elevation satellites (simultaneously in view, unless a more directive antenna is utilized); also given the older implementation of C/A tracking (even in current receivers), one would expect it to be noisier than the newer L2C code.

One problem associated with using S1/S2 measurements for snow sensing is that many receiver manufacturers only report these data to a precision of 1 dB (Bilich et al. 2007). Figure 2d shows the same data as in Fig. 2b, but the data have been decimated to 1 dB before converting to linear units. While the multipath modulations are still visible at the low elevation angles, the higher elevation angle data are severely degraded by this decimation. This negatively impacts how well one can retrieve the multipath frequency needed to estimate snow depth. Given that the SNR data are not directly valuable for positioning, it is understandable that receiver manufacturers have often neglected to provide better SNR precision to users. However, geodesists can certainly request access to better SNR data, as they are most certainly being generated by all carrier phase tracking receivers. The receiver used in this study (Trimble NetRS) generates SNR at a precision of 0.1 dB. Updates to the RINEX specification have improved the situation, by suggesting—although still not mandating—that S1/S2 observations be reported in dB–Hz and also by providing new observable identifiers to different signals in the same frequency (e.g., S2X and S2Y).

Fig. 2 a Recorded L2C SNR data for a rising arc for PRN 25 at PBO receiver p101; **b** rising arc of PRN 25 SNR data below elevation angle of 30°, second-order polynomial removed and converted from dB to linear units (for simplicity, volts); **c** SNR L1 C/A data for PRN 25 and L2P data for PRN 18, converted as in **b**). The L2P SNR data have been scaled by a factor of five. PRN 18 has a similar azimuth as PRN 25; **d** same as data in (**b**), with SNR data rounded to 1 dB

The GPS footprint and sensitivity of GPS data to snow depth

Most geodesists are used to visualizing satellite tracks in a polar projection ("sky plot"). For multipath studies, it is more helpful to plot the nominal specular reflection point on the local horizontal plane surrounding the antenna. This emphasizes the directions of the tracks as they will appear on the ground and gives some intuition about the spatial extent of the method. The radial distance of the reflection point is just the antenna height divided by the tangent of the elevation angle. Azimuth is simply the azimuth angle of the satellite transmitter with respect to the GPS site. As the multipath signal is dominated by data from low elevation angles, Fig. 3 shows the reflection points for the 8 healthy L2C satellites and elevation angles below 25° (PRN 5, 7, 12, 15, 17, 25, 29, and 31). It would seem as if any of these ground tracks could be used to estimate snow depth provided the surface is nearly planar. However, this analysis is restricted to satellites that at least rise up to a certain elevation angle (20° in this study), so that there are sufficient data to estimate the frequency of the multipath modulation. For example, the track for PRN 31 in the northwest quadrant is not used in this study. One can also see that for this site, two southern tracks (PRN 29 and 17) do not extend to 5°. This is not due to obstructions, but rather to tracking restrictions for the receiver used by PBO (12 channels). Geodetic receivers are typically programmed to track the satellites that are at the highest elevation angles. This means that data for some of the L2C tracks are not consistently available below 10°.
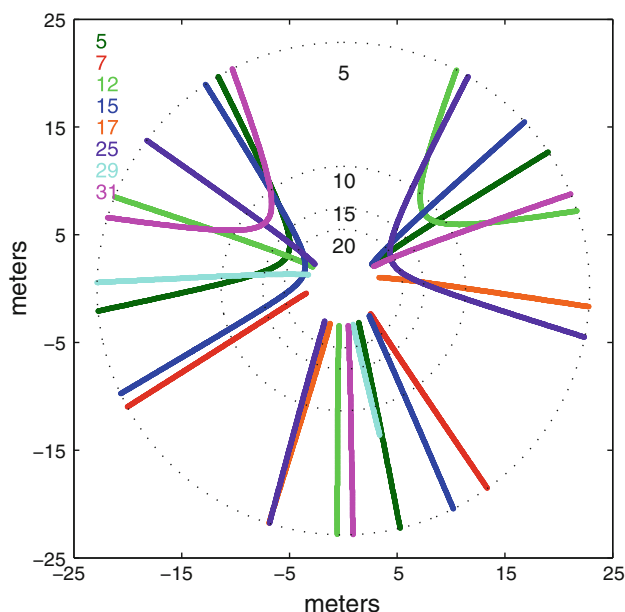
Figure 3 identifies the reflection point for each satellite track; this is not the same as the sensing footprint of the method. The GPS footprint for a flat surface with negligible roughness can be derived from the bistatic radar literature as the first Fresnel zone (FFZ; see, e.g., Katzberg et al. 2006, and "Appendix"). Compared to space or airborne platforms, where the FFZ might be many square kilometers, the FFZ in ground-based installations is much smaller. For a nominal horizontal surface, it fundamentally depends on the height of the antenna above the reflecting surface and the elevation angle between the satellite and the local horizon at the antenna: the FFZ gets larger with increasing antenna height. In shape, the FFZ is an elongated ellipse, ~4 m across in the direction perpendicular to satellite azimuth, more or less independent of elevation angle. The FFZ is substantially longer in the radial direction, especially near-grazing incidence. Figure 4a shows FFZ for an antenna 2-m high for elevation angles from 7 to 25°. Although not universal, 2 m is the most common antenna height in the PBO network. Figure 4b shows the FFZ for the same antenna but assuming that there is 1 m of snow on the ground. Because the GPS signal essentially reflects off the top of the snow in this case, the FFZ is significantly smaller for snow-covered ground than for bare ground. The FFZ for all elevation angles is also closer to the antenna. For regions with large snow depth variations, the footprint in late winter could be ~30% smaller than in early winter. Even so, the smaller GPS sensing zone still provides a much larger spatial average than that of SNOTEL (10 m^2).

The fundamental requirement of GPS snow sensing is that the area surrounding the GPS antenna must act as a specular reflector (Larson et al. 2009; Ozeki and Heki 2012). For this to occur, it suffices that the surface be nearly planar, large enough to encompass the FFZ at lower elevation angles, and free of substantial vegetation. A detailed explanation of the model for GPS multipath based
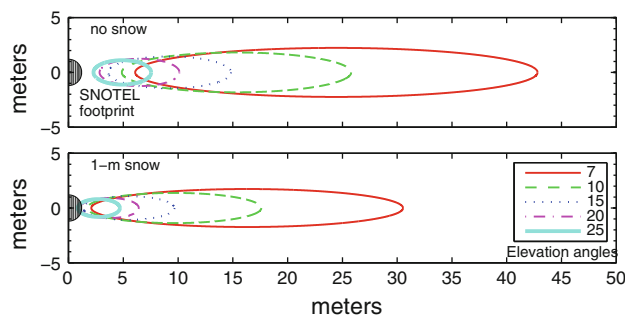

Fig. 3 Multipath reflection points for L2C satellites recorded at PBO site p360 on July 19, 2011

Fig. 4 First Fresnel zones for a satellite rising from the east are depicted for elevation angles from 7 to 25°. Antenna height is set at 2 m for both figures. In the *top panel*, no snow is present. In the *lower panel*, the Fresnel zone is computed for a meter of snow. The snow-sensing zone for each GPS site could in principle include one of these Fresnel zones for each ground tracks shown in Fig. 3. Half of the SNOTEL footprint is shown centered at zero

Fig. 5 Effect of terrain slopes (degrees) on snow depth retrievals
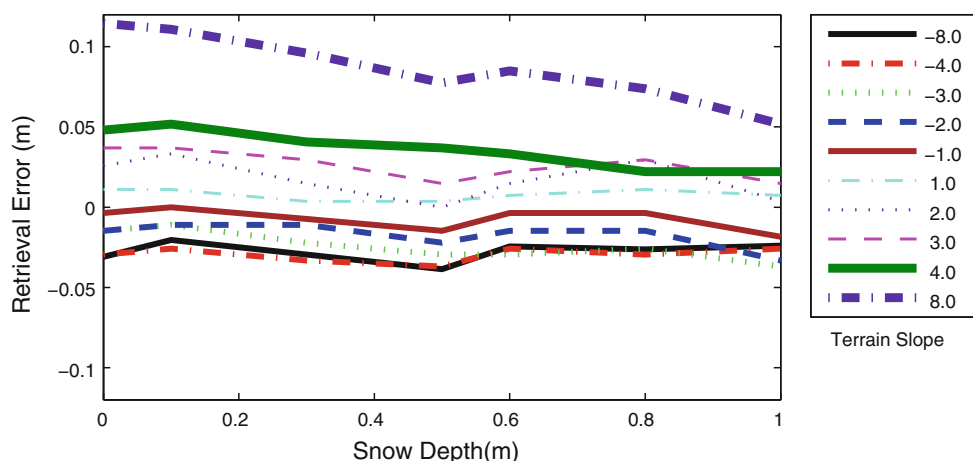
on geodetic antennas and planar-layered media can be found in Zavorotny et al. (2010). Example model predictions for snow effects were also given in Larson et al. (2009). The key point for snow sensing is that the dominant GPS reflection is at the air-snow interface. For horizontal planar reflectors and the antenna used by PBO (choke ring), the multipath modulation frequency is constant for sine of the satellite elevation angle e, meaning detrended SNR signals can be modeled very simply as a sinusoid:

$$SNR - P_d - P_r = A \cos\left(4\pi h\lambda^{-1} \sin e + \varphi\right) \quad (2)$$

The amplitude A will represent an average of the variable factor $\sqrt{P_d P_r}$ over the arc span. The parameter h is the vertical distance between the antenna phase center and the snow surface; λ is the GPS carrier wavelength (for the L2 frequency, it will be ~ 24.4 cm). Snow depth is just defined as:

$$\text{Snow depth} = (\text{vertical distance to the ground}) \\ - (\text{vertical distance to the snow layer}) \quad (3)$$

The first term is the vertical distance between the antenna and the *sensed* ground; it cannot be assumed equal to the height of the antenna above the ground immediately under it—it will be greater downhill and smaller uphill. While there are many planar surfaces near PBO sites, none is completely horizontal. Even small ground tilting angles translate into several tens of centimeters at the large horizontal distances involved. In practice, one can use the SNR data to estimate the vertical distance to the ground, analogously to how the distance to the snow surface was estimated. This means that bare ground must be observed prior or posterior to it becoming snow-covered, in summertime then winter. Such a topographic bias remains stable over time as long as satellites have repeatable ground tracks, which fortunately is the case for GPS. It also remains relatively stable for varying snow depth. In order to evaluate the residual effect of small slopes (<10°), simulations were

ran for a 2-m antenna height with a variety of snow depth levels and terrain slopes (both positive and negative) (Fig. 5). For slopes of 8° and less, the error in snow depth retrieval is 2–5 cm, which is small compared to the snow depth signals of interest for the western United States.

Finally, while the frequency of the air-soil multipath reflection depends also on how wet the soil is, the variation in vertical distance to the ground from this effect is only 2–3 cm (Larson et al. 2010). Snow density also affects the multipath reflection, but it is a much smaller effect than the air-snow interface (Gutmann et al. 2011). It will be ignored in this study.

Evaluations of PBO sites for snow sensing

Figure 6 shows examples of how snow depth can—and cannot—be estimated from GPS SNR data. On the top panel are shown three SNR traces from PBO site p101. The dates of these data were specifically chosen to represent conditions when no snow was on the ground and ~ 50 and 100 cm of snow was on the ground. A Lomb-Scargle periodogram (LSP) was computed for each SNR trace shown (Press et al. 1996). On each day, the retrieved frequencies have been converted to a reflector height (Eq. 2). The changes in reflector height are pronounced for this satellite track, and the peaks are much greater than the background LSP noise, indicating a strong specular reflection. In the second panel, results are shown for site p360. Again, there are strong peaks, although on day of year 300, the LSP estimate is weakened by missing SNR data. Contrast this with the results shown in the next two panels for sites p711 and p720. The SNR traces show no obvious reflector modulation frequency on any of the 3 days. The LSP plot confirms that there is no strong reflector at ~ 2 m, where it would be expected. Note the difference in the frequency content in the SNR data for p711 and p720.

Fig. 6 a–d SNR data for representative tracks at sites p101, p360, p711, and p720. Day of year 300 (2010) represents bare soil reflections; day of year 330 (2010) and 80 (2011) represent days with low and high snow levels. Lomb-Scargle periodograms computed for the SNR data are shown in the *right panels* in plots (**e–h**)
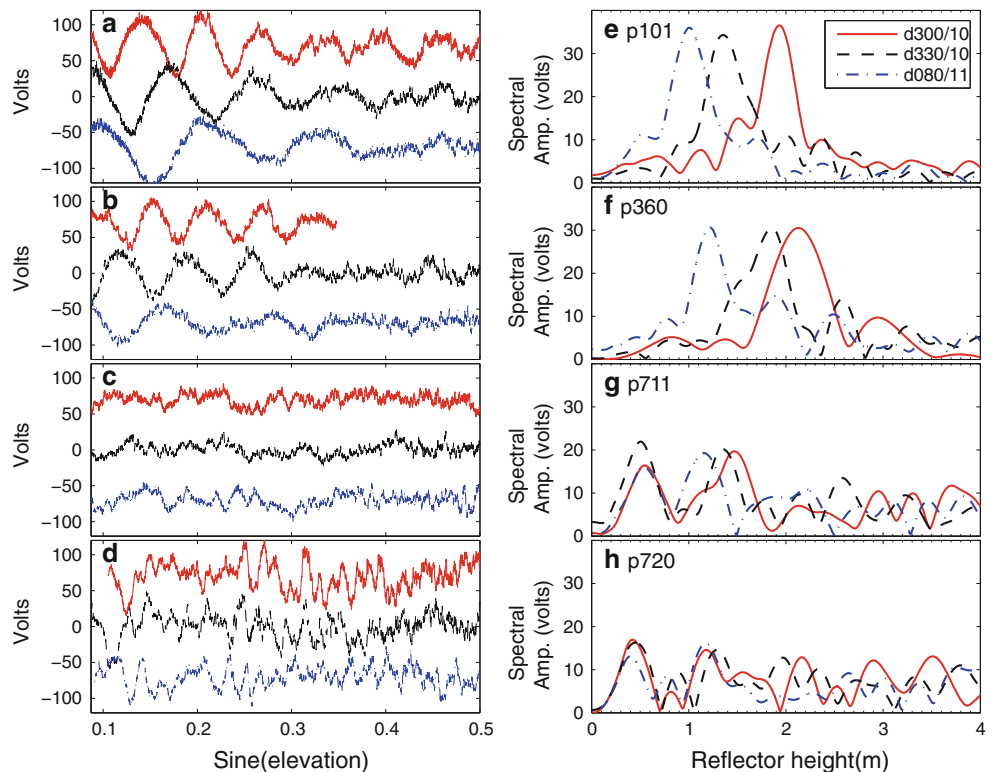
The discrepancies between the qualities of retrieval at these sites could be due to a variety of factors, including ground roughness and vegetation cover. Photographs indicate that the ground at site p360 is not particularly smooth on a small scale, but it is very flat over the sensing zone. Local slope calculations at p101 (a successful snow-sensing site) and p711 (an unsuccessful site) suggest that terrain variation is not the primary factor (Fig. 7). In fact, site p101 has much greater variation in local slope than p711. However, trees can also block ground reflections. The photographs (Fig. 7) indicate that unlike p101, site p711 is in a forested region. A satellite image of p711 (Fig. 8) confirms that there are blockages from trees in nearly all directions. An examination of photographs and Google Earth images confirms that p720 is also in a forested region. It is also obstructed by local topography, yielding very few measurements below 15°.

Except for completely flat and unobstructed regions, the quality of different satellite tracks will vary at each site. Although p101 has strong reflections in some directions (Fig. 6), it also has complex reflections in others (Fig. 9). The SNR data for this track show both a low-frequency peak consistent with ground reflections from 2 m and significant high-frequency content. This track is in the northeast quadrant. The local slope calculations indicate that there is a rise to the northeast, with a slope of nearly 16° at a distance of ∼100 m. The presence of high-frequency signals in the SNR data is a diagnostic of far

reflectors (Bilich and Larson 2007). In order to use data with these complex reflections for snow sensing, 1 Hz sampled GPS data would be required to extract and remove the high-frequency signal; otherwise, their neglect would translate into increased noise levels (Fig. 5).

Snow depth retrievals

In the northern summer of 2011, PBO turned on L2C tracking at over 900 sites. Before that time, it had enabled L2C for only a handful of sites. This initial period was used to assess the impact of L2C tracking on the primary PBO science data, the L1 and L2 carrier phases. For this reason, only limited results can be shown at this point. Each site used in this study was operating at 1 Hz. Results for three sites (p360, p684, and p030) are available for two water years (October 1–September 30), and p101 results are available for one. The data were analyzed as follows:

1. Initially satellite tracks were chosen by evaluating Lomb-Scargle periodograms (LSP). Only tracks with strong ground reflections were further analyzed on a daily basis.
2. Daily SNR data files were separated by rising and setting satellite tracks. Tracks that crossed midnight were completed by concatenating 2 days of data. LSPs were computed for data between elevation angles 5 and 30°. Tracks without 2,000 points or where peaks
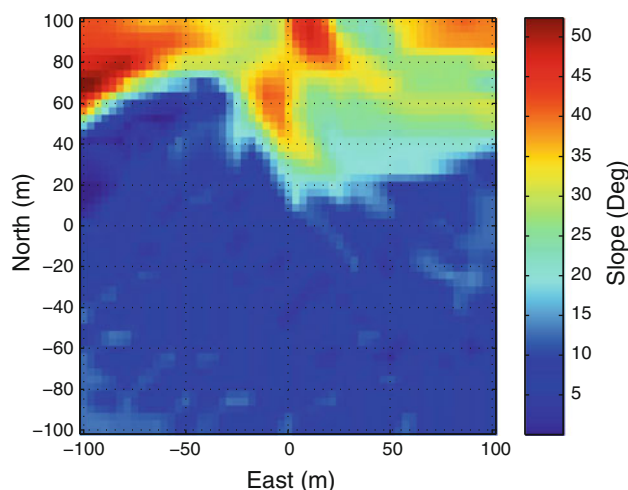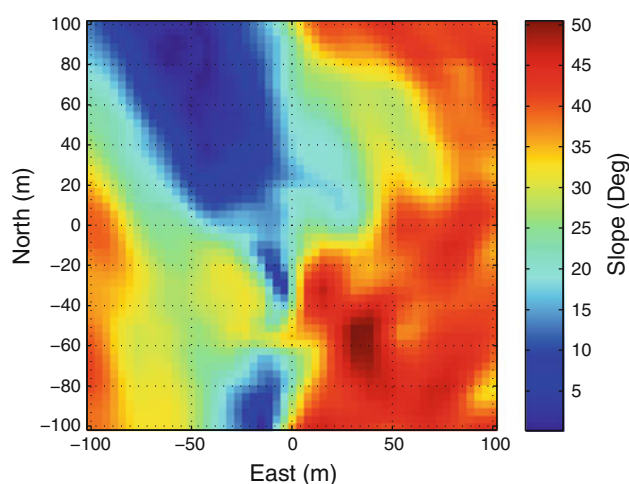
Fig. 7 Photograph and local terrain slopes for PBO site p101 (*left*) and site p711 (*right*)

did not exceed 4 times the background noise were discarded.

3. Summertime data were used to estimate the average height of the antenna above snow-free soil.

4. Snow depth was estimated each day for each valid satellite track by subtracting the LSP antenna height from the soil height determined in step 3.

5. Each day a mean snow depth was calculated from the output of step 4. A formal error was determined by calculating the standard deviation for all available tracks. The total error includes an error of 2.5 cm, added in quadrature, representing uncertainty in the average height of the antenna above bare soil.

Figure 10a shows GPS snow depth estimates for site p360 in eastern Idaho (Fig. 1c). The flattest site described in this study, on average over 10 tracks from the southern
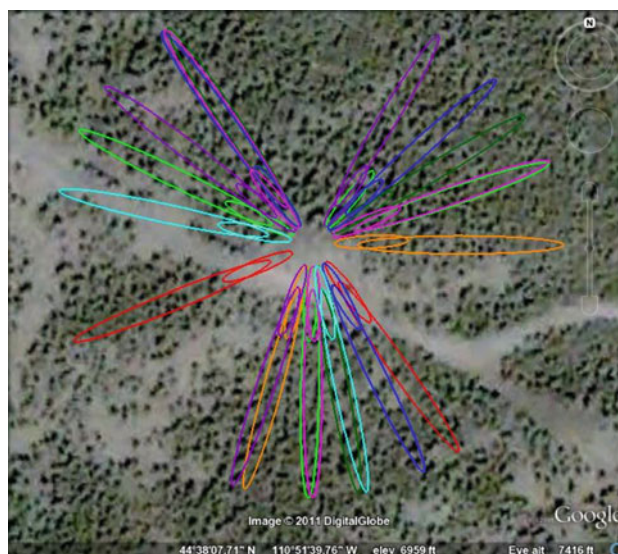
Fig. 8 Google Earth image for PBO site p711. Extent of Fresnel zones for L2C satellites and elevation angles of 5° also shown

azimuths, could be used to estimate snow depth on each day. The small error bars (2–3 cm) indicate that there was not significant azimuthal asymmetry in snow deposition at this site. In the 2009–2010 water year, GPS snow depth peaked at 0.8 m in early February. Also shown are SNOTEL snow depth records from Island Park, Idaho located 15 km from p360. It is also significantly higher in elevation (~60 m), and one would thus expect higher levels of snowfall. Indeed, peak snowfall at Island Park is ~20% higher than at p360. The GPS and SNOTEL closely track the same snow events, in that there are significant changes in snow depth at the same times. There is one late spring snowstorm in early April of 2010, followed by significant snowmelt over the next 30 days. The 2010–2011 water year shows 20% higher GPS snow depth estimates than the previous year. This is consistent with record snow levels reported for the Rocky Mountains last year. Snow was on the ground for almost 20 days longer than in the previous year. SNOTEL levels are higher in 2010–2011, but again show broad agreement with the timing of the snowstorms observed in the p360 data.

Figure 10b shows snow depth records for p101, located ~300 km south of p360 (Fig. 1c). SNOTEL records for Bug Lake, Utah, are also shown. This site is 15 km from p101 and over 400 m higher in elevation; one would expect significantly higher snow depth levels for the SNOTEL site than for p101. GPS snow depths peak at ~1.2 m in March. SNOTEL records higher snow depth levels—more than 2 m—until April before starting to decline. Snow has melted at p101 by April, but remained at Bug Lake until late June.

Figure 11a and b shows PBO snow depth records for sites p030 and p684. The former is in western Wyoming, ~50 km from p101. The latter is about the same distance from p360. Snow depth levels at these sites show significant temporal and spatial variability, both inter- and intra-site (the latter reflected in the error bars). Snow levels at p684 are quite similar between the 2 years. Abrupt changes in snow depth at p684 correspond to snowstorms visible in the two previous comparisons. Snow depth at p030 was significantly higher in year 2 than in year 1. Unlike p360 and p101 where snow took weeks to melt, snow melts quickly at p030 in both 2010 and 2011. An evident snowstorm at 2010.25 appears to be an outlier in the GPS analysis, but note that it corresponds to snowstorms in the SNOTEL records shown in Fig. 10.

Conclusions

Information about the extent and depth of snow is of great importance for studies of the earth's climate system. Snow data are also needed to improve forecasts of, and therefore
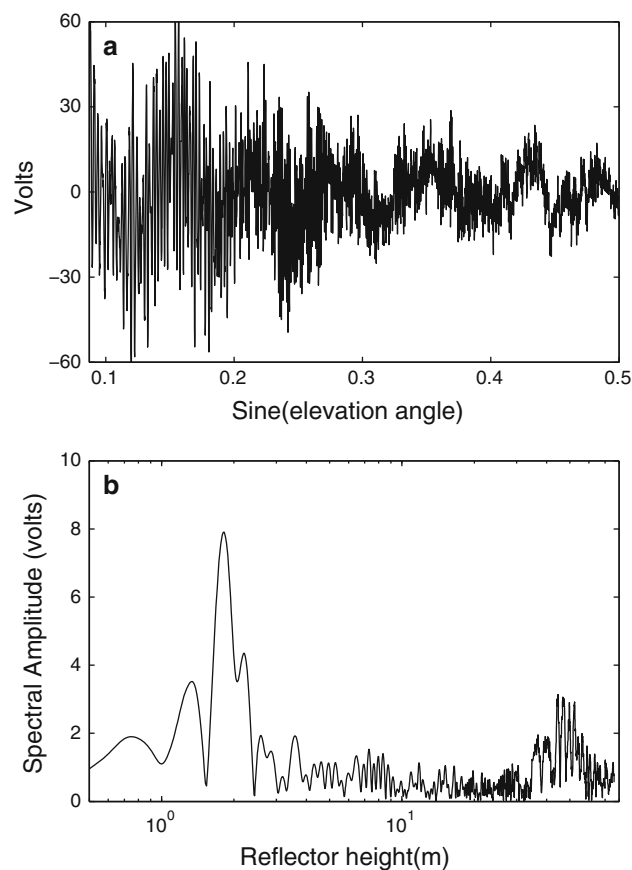

Fig. 9 *Top* GPS SNR data for PRN 31 in NE quadrant at PBO station p101; *bottom* Lomb-Scargle periodogram of data in *top panel*

mitigate the effects of, natural hazards such as droughts and floods. Although networks exist to measure snow parameters, no one network can measure snow quantities at the needed spatial and temporal scales. Using data from the EarthScope Plate Boundary Observatory, we demonstrate that GPS receivers installed to measure deformation associated with plate tectonics can also be used to estimate snow depth on a daily basis. The footprint of these snow estimates (hundreds of square meters) is intermediate to existing in situ sensors (SNOTEL) and intermittently measured snow courses. The GPS snow depth estimates could also be valuable for validating future satellite observations of snow depth/extent. These estimates utilize the SNR data that are routinely included with the carrier phase observables in data archived by geodesists and surveyors.

This study benefited from excellent descriptions of each site provided by the PBO network operators. In particular, multiple photographs were routinely available for each site, providing invaluable information about the local reflection environment. Augmented with Google Earth images and publicly available digital elevation maps, it was straightforward to evaluate the potential of each site for snow sensing.

Fig. 10 GPS snow depth retrievals from PBO sites p360 and p101. Standard deviations represent the standard deviation of the individual satellite tracks and a formal error of 2.5 cm, added in quadrature. SNOTEL data are also shown
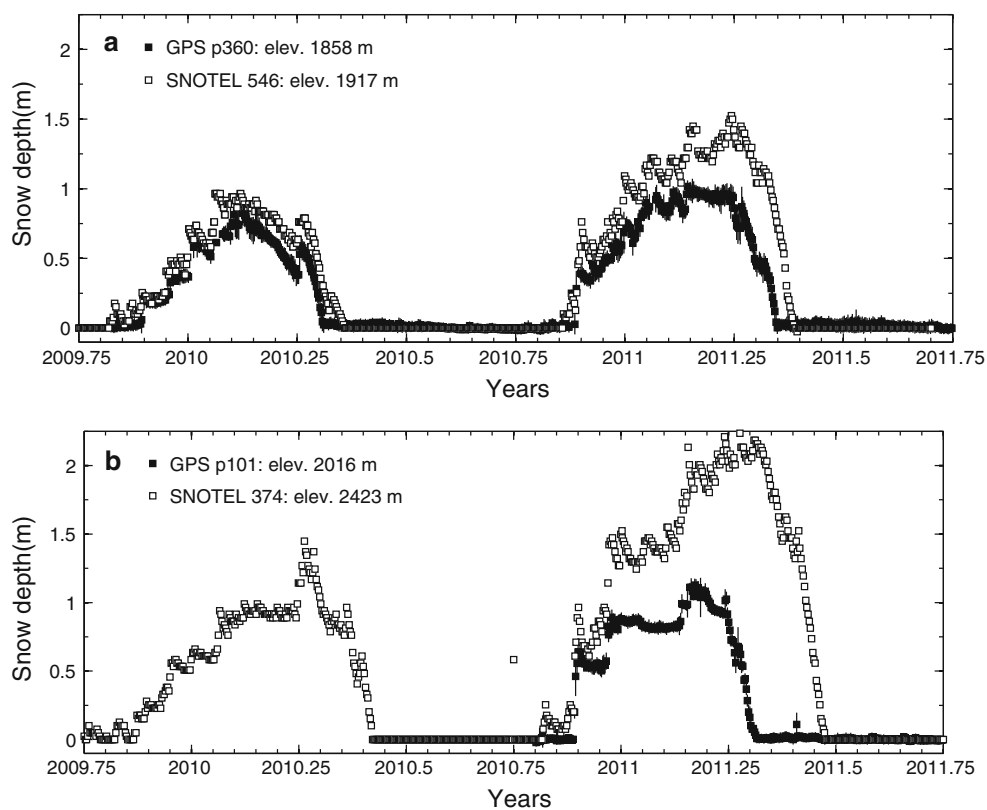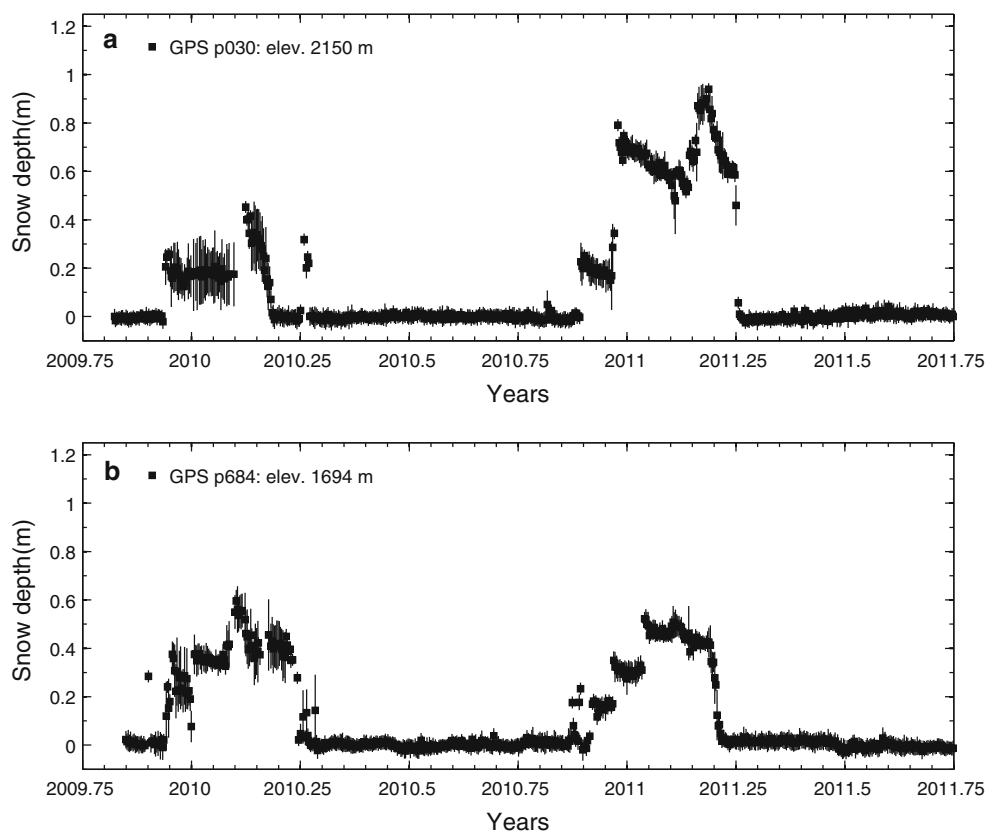

Fig. 11 GPS snow depth retrievals from PBO sites p030 and p684. Standard deviations represent the standard deviation of the individual satellite tracks and a formal error of 2.5 cm, added in quadrature

Geodesists have invested hundreds of millions of dollars to install multiuser GPS networks for monitoring plate motions, volcano deformation, and precipitable water vapor. Surveyors also operate large GPS networks to maintain geodetic control within states and counties. This study demonstrates that for GPS networks outside urban settings, snow depth is straightforward to measure using existing infrastructure. It also suggests that the future expansion of GPS infrastructure should take into account the multiuse potential of GPS networks, meaning that sites can be chosen that produce both good positions and good snow depth estimates.

Appendix

To avoid confusion with Fresnel zones expressions valid for space- and air-borne platforms, here we provide expressions for ground-based installations (Hristov 2000). Start with $n = 1$ indicating the first Fresnel zone (FFZ), λ for wavelength, h for antenna height, and e and a for satellite elevation angle and azimuth, respectively. Then, the FFZ dimensions are:

$$d = n\lambda/2;$$
$$R = h/\tan(e) + (d/\sin(e))/\tan(e)$$
$$b = (2\ d\ h/\sin(e) + (d/\sin(e))^2)^{1/2}$$
$$a = b/\sin(e)$$

Its perimeter can be discretized as function of the inner angle $\theta \in [0, 2\pi]$:

$$x' = a\ \cos(\theta) + R$$
$$y' = b\ \sin(\theta)$$

Finally, the semi-major axis is aligned with the satellite azimuth:

$$x = \sin(a)\ x' - \cos(a)\ y'$$
$$y = \sin(a)\ y' + \cos(a)\ x'$$

References

Armstrong RL, Brodzik MJ (2002) Hemispheric-scale comparison and evaluation of passive-microwave snow algorithms. Ann Glaciol 34:1:38–44 (7). doi:10.3189/172756402781817428

Bilich A, Larson KM (2007) Mapping the GPS multipath environment using the signal-to-noise ratio (SNR). Radio Sci 42:RS6003. doi:10.1029/2007RS003652

Bilich A, Axelrad P, Larson KM (2007) Scientific utility of the signal-to-noise ratio (SNR) reported by geodetic GPS receivers. Proceedings of the 20th international technical meeting of the satellite division of the institute of navigation (ION GNSS 2007), Fort Worth, TX, Sep 2007, pp 1999–2010

Bloschl G, Kirnbauer R, Gutknecht D (1991) Distributed snowmelt simulations in an alpine catchment: 1. Model evaluation on the basis of snow cover patterns. Water Resour Res 27:3171–3179

Elder K, Dozier J, Michaelsen J (1991) Snow accumulation and distribution in an alpine Watershed. Water Resour Res 27:1541–1552

Erickson T, Williams MW, Winstral A (2005) Persistence of topographic controls on the spatial distribution of snow depth in rugged mountain terrain, Colorado, USA. Water Resour Res 41(4):W04014. doi:10.1029/2003WR002973

ESA (2008) CoReH2o—COld REgions hydrology high-resolution observatory, ESA SP-1313/3 candidate earth explorer core missions—report for assessment

Gutmann E, Larson KM, Williams M, Nievinski FG, Zavorotny V (2011) Snow measurement by GPS interferometric reflectometry: an evaluation at Niwot Ridge, Colorado. Hydrol Process. doi:10.1002/hyp.8329

Hristov HD (2000) Fresnel zones in wireless links, zone plate lenses and antennas. Artech House. ISBN 9780890068496, pp 323

Jaldehag KRT, Johansson JM, Davis JL, Elósegui P (1996) Geodesy using the Swedish permanent GPS network: effects of snow accumulation on estimates of site positions. Geophys Res Lett 23(13):1601–1604

Joseph A (2010) What is the difference between SNR and C/N0? InsideGNSS, Nov/Dec 2010, pp 20–25

Katzberg S, Torres O, Grant M, Masters D (2006) Utilizing calibrated GPS reflected signals to estimate soil reflectivity and dielectric constant: results from SMEX02. Rem Sens Environ 100(1):17–28

Kind RJ (1981) Snow drifting. In: Gray D, Male D (eds) Handbook of snow: principles, processes, management and use. Elsevier, New York, pp 338–359

Larson KM, Gutmann E, Zavorotny V, Braun JJ, Williams M, Nievinski FG (2009) Can we measure snow depth with GPS

receivers? Geophys Res Lett 36:L17502. doi:10.1029/2009 GL039430

Larson KM, Braun JJ, Small EE, Zavorotny V, Gutmann E, Bilich A (2010) GPS multipath and its relation to near-surface soil moisture. IEEE-JSTARS 3(1):91–99. doi:10.1109/JSTARS. 2009.2033612

Molotch N, Bales R (2006) SNOTEL representativeness in the Rio Grande headwaters on the basis of physiographics and remotely sensed snow cover persistence. Hydrol Process 20:723–739

Ozeki M, Heki K (2012) GPS snow depth sensor with geometry-free linear combinations. J Geod 86(3):209–219. doi:10.1007/ s00190-011-0511-x

Press F, Teukolsky S, Vetterling W, Flannery B (1996) Numerical recipes in Fortran 90: the Art of parallel scientific computing, 2nd edn. Cambridge University Press, Cambridge

Serreze MC, Clark MP, Armstrong RL, McGinnis DA, Pulwarty RS (1999) Characteristics of the Western United States snowpack from snowpack telemetry (SNOTEL) data. Water Resour Res 35(7):2145–2160

Seyfried MS, Wilcox BP (1995) Scale and the nature of spatial variability: field examples having implications for hydrologic modeling. Water Resour Res 31:173–184

Woo KT (1999) Optimum semi-codeless carrier phase tracking of L2. In: Proceedings of the 12th international technical meeting of the satellite division of the institute of navigation, Nashville, TN., Sep 14–17, 1999

Zavorotny V, Larson KM, Braun JJ, Small EE, Gutmann E, Bilich A (2010) A physical model for GPS multipath caused by ground reflections: toward bare soil moisture retrievals. IEEE-JSTARS 3(1):100–110. doi:10.1109/JSTARS.2009.2033608

Author Biographies

Dr. Kristine M. Larson is a Professor of Aerospace Engineering Sciences at the University of Colorado. Her current research focuses on GPS reflections.

Felipe G. Nievinski is a Ph.D. candidate at the Department of Aerospace Engineering Sciences at the University of Colorado.